Available online at ScienceDirect

Resuscitation

journal homepage: www.elsevier.com/locate/resuscitation

Experimental paper

Low frequency power in cerebral blood flow is a biomarker of neurologic injury in the acute period after cardiac arrest

Brian R. White[a,*], *Tiffany S. Ko*[b], *Ryan W. Morgan*[c], *Wesley B. Baker*[b], *Emilie J. Benson*[d], *Alec Lafontant*[b], *Jonathan P. Starr*[c], *William P. Landis*[c], *Kristen Andersen*[b], *Jharna Jahnavi*[b], *Jake Breimann*[b], *Nile Delso*[c], *Sarah Morton*[c], *Anna L. Roberts*[c], *Yuxi Lin*[c], *Kathryn Graham*[c], *Robert A. Berg*[c], *Arjun G. Yodh*[d], *Daniel J. Licht*[b], *Todd J. Kilbaugh*[c]

Abstract

Aim: Cardiac arrest often results in severe neurologic injury. Improving care for these patients is difficult as few noninvasive biomarkers exist that allow physicians to monitor neurologic health. The amount of low-frequency power (LFP, 0.01–0.1 Hz) in cerebral haemodynamics has been used in functional magnetic resonance imaging as a marker of neuronal activity. Our hypothesis was that increased LFP in cerebral blood flow (CBF) would be correlated with improvements in invasive measures of neurologic health.

Methods: We adapted the use of LFP for to monitoring of CBF with diffuse correlation spectroscopy. We asked whether LFP (or other optical biomarkers) correlated with invasive microdialysis biomarkers (lactate-pyruvate ratio – LPR – and glycerol concentration) of neuronal injury in the 4 h after return of spontaneous circulation in a swine model of paediatric cardiac arrest (*Sus scrofa domestica*, 8–11 kg, 51% female). Associations were tested using a mixed linear effects model.

Results: We found that higher LFP was associated with higher LPR and higher glycerol concentration. No other biomarkers were associated with LPR; cerebral haemoglobin concentration, oxygen extraction fraction, and one EEG metric were associated with glycerol concentration.

Conclusion: Contrary to expectations, higher LFP in CBF was correlated with worse invasive biomarkers. Higher LFP may represent higher neurologic activity, or disruptions in neurovascular coupling. Either effect may be harmful in the acute period after cardiac arrest. Thus, these results suggest our methodology holds promise for development of new, clinically relevant biomarkers than can guide resuscitation and post-resuscitation care.

Institutional protocol number: 19-001327.

Keywords: Cardiac arrest, Diffuse correlation spectroscopy, Low frequency power, Microdialysis, Optical neuromonitoring

Introduction

Cardiac arrest affects approximately 300,000 adults and 15,000 children in the United States annually.[1] Despite improvements in survival, poor neurological outcomes remain common.[2–4] Neurologic monitoring during early recovery could improve prognostication and implementation of targeted neuroprotective strategies;[5,6] however, many such methods are invasive. Noninvasive optical neuromonitoring methods (e.g., near infrared spectroscopy or diffuse optical spectroscopy, DOS) are attractive, but to-date they only indirectly detect neurologic injury via effects on oxygen saturation.[7] Measurement of

Abbreviations: BFI, blood flow index, CBF, cerebral blood flow, DCS, diffuse correlation spectroscopy, DOS, diffuse optical spectroscopy, LFP, low frequency power, THC, total haemoglobin concentration

* Corresponding author at: Room 907C, 3615 Civic Center Blvd., Philadelphia, PA 19104, United States.
E-mail address: whiteb1@chop.edu (B.R. White).

https://doi.org/10.1016/j.resuscitation.2022.07.004
Received 8 March 2022; Received in Revised form 29 June 2022; Accepted 4 July 2022
Available online xxxx

signatures of neuronal activity in cerebral haemodynamics would enable more comprehensive assessment of neurologic metabolism. In this contribution, we adapt a neuronal activity metric from functional magnetic resonance imaging (fMRI) called low frequency power (LFP) and apply it to non-invasive optical monitoring of cerebral blood flow (CBF).

The temporal properties of cerebral haemodynamics reflect neuronal activity through neurovascular coupling. Canonically, a stimulus results in a rise in CBF, blood volume, and blood oxygenation.[8–9] However, the brain is highly metabolically-active even at rest, accounting for 20–30% of the body's energy consumption.[10–11] Seemingly random fluctuations in cerebral haemodynamics reflect this resting-state brain activity, with vascular changes primarily driven by low frequency local field potentials, usually analyzed in the range of ~0.01–0.1 Hz.[10] Most famously, analysis of resting-state brain activity is used in functional connectivity, where correlation analysis identifies functional networks.[12–14] In addition, the amount of low frequency signal has been used in fMRI and optical neuroimaging as a proxy for the amount of local neuronal activity.[15–17].

Notably, LFP of CBF fluctuations, measured by transcranial Doppler (TCD) of the middle cerebral artery correlated with neurologic recovery in the days after cardiac arrest.[18] Our objective in the present work was to use a piglet model of paediatric cardiac arrest and optical diffuse correlation spectroscopy (DCS, a measure of microvascular CBF) to assess LFP as a biomarker of neurologic injury in the acute period after cardiac arrest (up to 4 h post-recovery). Our hypothesis was that higher LFP in the DCS signal (as a presumed proxy for neuronal activity) would correlate with improved invasive biomarkers of neurologic injury obtained from microdialysis.

Methods

Cardiac arrest model

We used an established paediatric porcine asphyxial cardiac arrest model. All procedures were approved by the Institutional Animal Care and Use Committee (IACUC) of the Children's Hospital of Philadelphia and performed in accordance with the National Research Council's "Guide for the Care and Use of Laboratory Animals", the PHS Policy on Humane Care and Use of Laboratory Animals, and the USDA Animal Welfare Act. The experiment is reported according to the ARRIVE guidelines. The protocol was not pre-published or registered.

The model has been described elsewhere.[19–21] One-month-old swine (*Sus scrofa domestica*, 8–11 kg) were anesthetized and endotracheally intubated. Baseline monitoring was performed for five minutes. Asphyxia was induced by endotracheal tube clamping. After seven minutes, ventricular fibrillation was induced by electrical pacing. The endotracheal tube was then unclamped and haemodynamic-directed CPR[19–22] with manual chest compressions was performed. As part of a larger study, these animals were randomized to one of two CPR strategies: (1) compression depth titrated to maintain a systolic aortic blood pressure (SBP) of 90 mmHg and vasopressor administration titrated to maintain a diastolic aortic blood pressure (DBP) above 30 mmHg, and (2) resuscitation titrated to higher targets (SBP of 110 mmHg. DBP above 40 mmHg). CPR was performed for up to 20 min with eligibility for cardiac defibrillation beginning in the tenth minute. The present study is a retrospective observational analysis. The researchers performing the present analysis were blinded to the clinical state of the animals and any prior study data.

Animals who achieved return of spontaneous circulation (ROSC) were monitored for four hours (Fig. 1A) and survived to 5 days. During the monitoring period, care consisted of mechanical ventilation to maintain an end-tidal CO_2 of 38–42 mmHg and arterial oxygen saturation (by pulse oximetry) of 94–99%. Isoflurane was titrated to ensure absence of a toe-pinch reflex (requiring generally between 1% and 3%). Adrenaline (epinephrine) was used to maintain a mean arterial pressure (MAP) of at least 45 mmHg.

Optical neuromonitoring

Optical neuromonitoring was performed throughout using DOS and DCS. DOS data were acquired with a customized frequency-domain instrument (Imagent, ISS Inc., Champaign, IL) at 10 Hz with source-detector separations from 1.5 to 3.0 cm. DCS data were collected at 20 Hz using a custom-built instrument and a source-detector separation of 2.5 cm. These two modalities in a single probe were secured over the left frontal cortex (Fig. 1B). The instrument and initial pre-processing have been described previously.[21,23] DOS was used to calculate wavelength-dependent absorption and scattering coefficients and concentrations of oxy- and deoxy-haemoglobin. These values and DCS were used to calculate the blood flow index (BFI), a metric of CBF. Additional pre-processing included the removal of non-physiologic data points (total haemoglobin concentration (THC) below 25 μM or above 175 μM and BFI below 0 cm^2/s or above 10^{-7} cm^2/s).

To calculate LFP, data were assessed in five-minute moving intervals in five-second increments. Analysis was performed on intervals where ≥95% of time-points were present. Missing data were linearly interpolated. The Fourier transform was calculated, and LFP was the amount of power in the interval from 0.01 Hz to 0.1 Hz (assigned to the time-point at the end of the five-minute interval). After Fourier analysis, BFI was smoothed with a 30-second rolling median filter. Normalized (relative) versions of variables (e.g., rLFP) were obtained by dividing their value by the median obtained over the pre-asphyxial baseline.

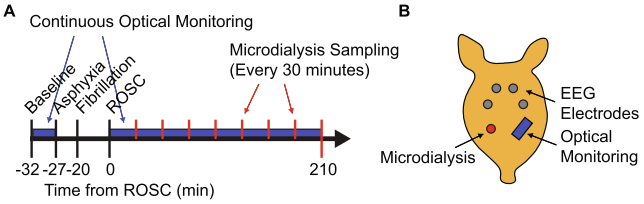

Fig. 1 – Experimental design of the post-arrest monitoring study. (A) After a baseline period, asphyxial cardiac arrest was induced by endotracheal tube clamping. Cardiopulmonary resuscitation was performed for up to 20 min. Return of spontaneous circulation (ROSC) was induced by defibrillation, if necessary. Animals that achieved ROSC were monitored for 4 h with continuous optical methods and EEG, and microdialysis was sampled every 30 min. (B) Diagram of the placement of neurologic monitoring on the head of the animals (viewed from above; the right side of the image is the left side of the animal).

The Imagent instrument collected data in 17.9 ± 2.2 second intervals interrupted by 1.14 second gaps. These large gaps in the data were not recoverable by interpolation. Thus, Fourier analysis was uninterpretable, and LFP of DOS was not performed. Concentrations for oxy- and deoxyhaemoglobin were calculated, and THC, tissue oxygen saturation (S_tO_2), and the oxygen extraction fraction (OEF) were derived. Calculation of OEF used an arterial oxygenation saturation obtained from pulse oximetry, the DOS-derived S_tO_2, and the venous sampling fraction (assumed to be 0.75).[23]

Electroencephalography

Electroencephalography (EEG) was performed with five electrodes (two channels and a reference) at 256 Hz. Channels were located on the left (C3-P3 according to the 10–20 system) and the right (C4-P4, Fig. 1B). Non-physiologic data (amplitude above 200 mV) was excluded along with a 10-second surrounding time period (to avoid artifacts from defilbrillation and filtering). An amplitude-integrated EEG (aEEG) was constructed using a low-pass filter (15 Hz), a high-pass filter (0.5 Hz), rectification, and a final low-pass filter (0.021 Hz).[24,25] To calculate the burst suppression ratio (BSR), the aEEG signals were divided into burst and suppressed intervals. Suppression was defined as an EEG amplitude below 5 mV for at least 2.4 s.[24,26] BSR was the fractional time spent in suppression in moving one-minute intervals.

Invasive biomarkers of neurologic injury

Cerebral microdialysis was performed in the right frontal cortex (CMA 71 Elite, mDialysis, Sweden) with a probe placed 0.5–1 cm deep in the brain parenchyma with the goal of placing it at the gray/white matter junction (Fig. 1B). Sterile saline was perfused at 1 μL/min, and equilibrated dialysate samples were collected in 30-minute intervals after ROSC. Samples were frozen, and pyruvate, lactate, and glycerol levels were subsequently analyzed (ISCUS Flex, mDialysis) as cerebral interstitial space measures of cerebral cellular energy metabolism (lactate, pyruvate) and cellular membrane degeneration (glycerol). Our primary outcomes were the lactate/pyruvate ratio (LPR) and glycerol concentration. In hypoxic conditions, or if mitochondrial function is compromised, pyruvate is metabolized to lactate; thus, LPR provides a robust measure of redox status with higher LPR indicating greater amounts of anaerobic metabolism. Higher glycerol indicates cellular membrane degeneration, likely corresponding to neuronal damage.[27]

Statistical analysis

The primary analysis (for which CPR strategy was not a variable of interest) assessed whether optical biomarkers (rBFI, rLFP, THC, and OEF) were correlated with the microdialysis outcome variables (LPR and glycerol) after ROSC. We also considered other possible physiologic biomarkers, including MAP, aEEG, and BSR. For inclusion, optical data had to be available for the baseline and after ROSC, and EEG and microdialysis data had to be available after ROSC. The median value for each variable was obtained over each interval of microdialysis collection. All variables were log-transformed prior to analysis. The correlation of each possible biomarker to each outcome was assessed using univariate linear mixed effects models (each biomarker was considered as a fixed effect with the addition of subject-specific random effects). Results are presented as the fixed effects estimator for each predictor (β) and a *p*-value.

Additionally, the above analyses were repeated examining only the animals in either the low- or high-target BP CPR cohorts. Furthermore, we asked whether any of the variables differed between the two CPR subgroups at any timepoint. For each 30 min interval, the values for every biomarker were compared between the low- and high-target BP cohorts using two-sample *t*-tests.

In a secondary analysis, we assessed the correlation between cerebral and systemic physiologic parameters with rLFP, performed as a series of univariable linear mixed effects models where the outcome variable was rLFP (predictors: rBFI, THC, OEF, rMAP, aEEG, and BSR). For this analysis, all piglets with both optical and EEG data after ROSC available were included. This analysis was repeated within each CPR subgroup.

All calculations were performed using MATLAB version 2020a (Mathworks, Natick, MA). All statistical tests were two-sided. An alpha level of 0.05 was assumed to represent statistical significance. A power calculation was not performed to generate the sample size. Rather, this was a convenience sample of available piglets from the larger study on CPR strategy.

Results

Thirty-seven piglets were considered for inclusion (57% female). Of these, twenty received CPR titrated to 90/30 mmHg and seventeen to 110/40. Three piglets (two high-target and one low-target) failed to achieve ROSC. In 11 piglets, microdialysis was not available (e.g., technical problems prevented analysis). Thus, 23 piglets were eligible for the primary analysis (comparing biomarkers to microdialysis) and 34 piglets were eligible for the secondary analysis (comparing rLFP to other physiologic parameters). For the primary analysis (where data was binned to match microdialysis), there were a median of 7 time-points per piglet (range: 6–7). For the secondary analysis, a median of 2652 time-points were available (interquartile range: 2519–2812).

The primary analysis compared microdialysis data with optical and physiologic variables. Relative low frequency power (rLFP) was the only biomarker correlated with LPR (Table 1, Fig. 2), with higher rLFP associated with higher LPR ($p = 0.019$). In contrast, rCBF and rMAP were not associated with LPR ($p = 0.35$ and 0.32, respectively). rLFP was also highly correlated with a higher glycerol level ($p = 0.0001$, Table 2). Again, rBFI and rMAP were not correlated with glycerol levels ($p = 0.11$ and 0.74, respectively). However, THC and OEF were corre-

Table 1 – Results of the univariate linear mixed effects models for prediction of the lactate-pyruvate ratio.

Prediction of lactate-pyruvate ratio (LPR)

Predictor	Regression coefficient (β)	*p*-value
Relative cerebral blood flow (rBFI)	−0.53	0.35
Relative low frequency power in cerebral blood flow (rLFP)	0.079	0.019
Total haemoglobin concentration (THC)	0.16	0.84
Oxygen extraction fraction (OEF)	0.16	0.70
Mean arterial blood pressure	−1.61	0.28
aEEG (Left)	0.40	0.35
aEEG (Right)	0.16	0.40
BSR (Left)	−0.009	0.55
BSR (Right)	−0.05	0.39

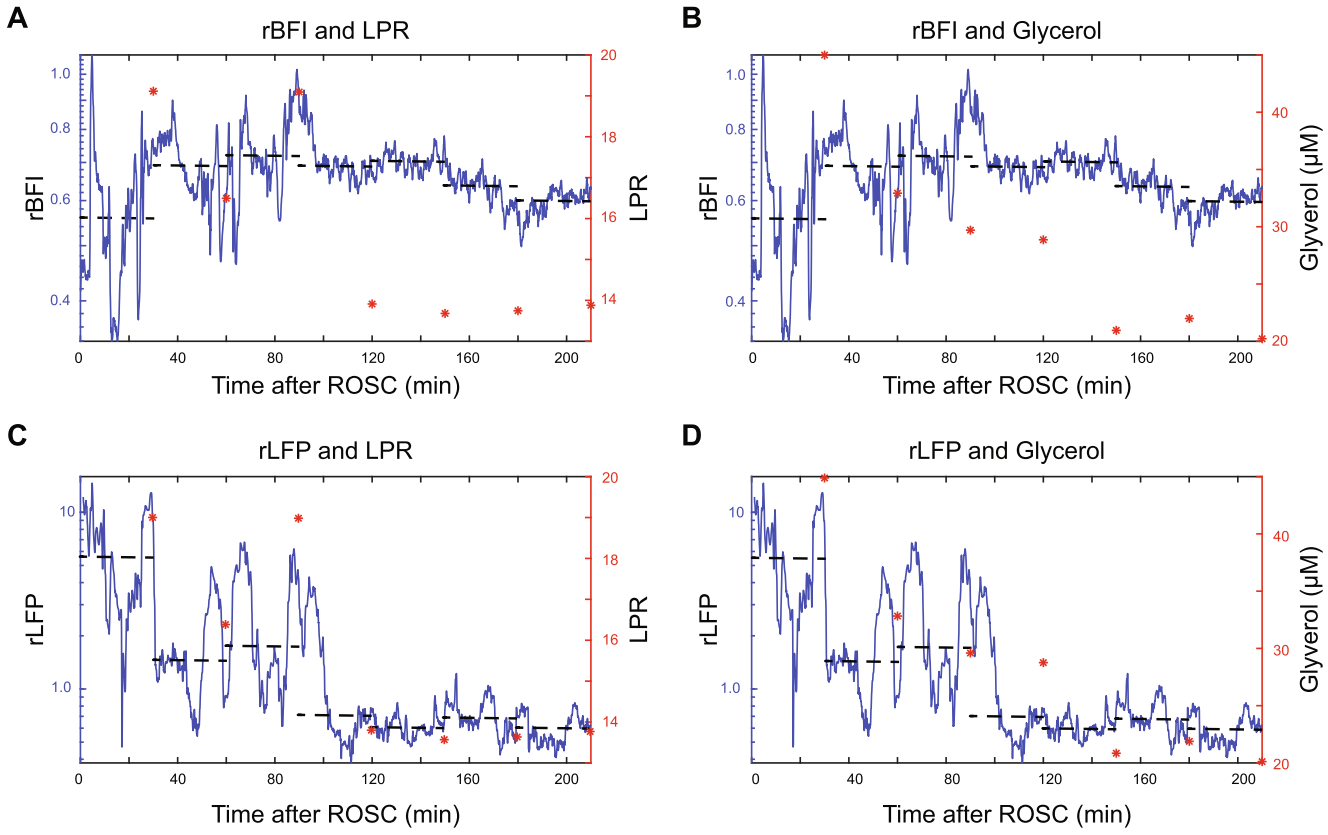

Fig. 2 – Example data (from a single piglet) after the return of spontaneous circulation (ROSC) demonstrating relative blood flow index (rBFI) and relative low frequency power (rLFP) and their relationship to lactate-pyruvate ratio (LPR) and glycerol concentration. The optical tracing is shown in blue with the median value of each 30-minute interval shown in black dashed lines (left-sided axis). The red stars show the microdialysis data (right-sided axis). (A–B) Comparison of rBFI with microdialysis data. There is substantial variability in BFI in the first hour after ROSC. But overall, notice that rBFI is low after ROSC before recovering and then slightly falling, which does not match the microdialysis time courses. (C–D) Comparison of rLFP with microdiaylsis. rLFP is initially volatile, but with a high median that decreases over time before stabilizing below baseline levels. This time course follows a similar time course to that from the microdialysis data.

lated with glycerol levels (p = 0.01 and 0.003, respectively). Higher BSR on the left (i.e., decreased neuronal activity) was associated with lower glycerol (p = 0.038); other EEG markers (including ipsilateral BSR) were not associated with glycerol.

Examining the two CPR subgroups individually, no predictors were associated with LPR (likely due to small sample sizes). In the low-target BP subgroup, rBFI, THC, and OEF were associated with glycerol concentration (p = 0.04, 0.008, and 0.04, respectively). In the high-target BP subgroup, rLFP, THC, and OEF were associated with glycerol concentration (p = 0.0001, 0.02, and 0.009, respectively). The only difference between the time courses of the two subgroups was that the low-target BP cohort had lower rBFI and rLFP (p = 0.04 and 0.03, respectively) at the 1-hour post-ROSC timepoint. The cohorts did not significantly differ in THC, OEF, MAP, any EEG variable, LPR, or glycerol at any time point.

We next assessed which variables were correlated with rLFP after ROSC. Greater rLFP was correlated with increased neuronal activity, as assessed by both higher aEEG (p = 0.003 and 0.04 for left and right, respectively) and lower BSR (p = 0.002 and <0.001, respectively, Table 3). rLFP was correlated with cerebrovascular physiology including increased rBFI, THC, and MAP (p < 0.001 for all three). Conversely, rLFP was not associated with OEF (p = 0.25). These same relationships held when examining the low- and high-target BP subgroups. In both cases, rLFP was associated with all EEG variables, rBFI, THC, and MAP. In the low-target BP cohort, rLFP was additionally associated with OEF.

Discussion

We found that LFP of CBF (obtained from DCS) was associated with two invasive biomarkers of neurologic injury obtained from microdialysis, higher LPR and higher glycerol, during the first four hours after cardiac arrest. No other optical or physiologic biomarkers were associated with LPR, and only increased THC, OEF, and lower contralateral BSR were associated with higher glycerol. These results demonstrate the promise of LFP as a biomarker of neurometabolic dysfunction during the post-resuscitation period.

LFP and its equivalent formulation, amplitude of low frequency fluctuations (ALFF), were developed for (blood oxygen level depen-

Table 2 – Results of the univariate linear mixed effects models for prediction of glycerol concentration.

Prediction of glycerol		
Predictor	Regression coefficient (β)	*p*-value
Relative cerebral blood flow (rBFI)	−0.36	0.11
Relative low frequency power in cerebral blood flow (rLFP)	0.20	0.0001
Total haemoglobin concentration (THC)	4.22	0.01
Oxygen extraction fraction (OEF)	2.61	0.003
Mean arterial blood pressure	0.31	0.48
aEEG (Left)	0.05	0.69
aEEG (Right)	0.0006	>0.99
BSR (Left)	−0.062	0.038
BSR (Right)	0.002	0.96

Table 3 – Results of the univariate linear mixed effects models for associations with relative low frequency power (rLFP).

Prediction of rLFP		
Predictor	Regression coefficient (β)	*p*-value
Relative cerebral blood flow (rBFI)	1.64	<0.001
Total haemoglobin concentration (THC)	6.36	<0.001
Oxygen extraction fraction (OEF)	−0.41	0.64
Mean arterial blood pressure	1.64	<0.001
aEEG (Left)	0.10	0.004
aEEG (Right)	0.10	0.003
BSR (Left)	−0.45	0.004
BSR (Right)	−0.46	<0.015

dent) BOLD-fMRI.[15] To date the neurologic underpinnings of LFP have not been fully elucidated, but haemodynamic fluctuations have been linked to local field potentials.[28,29] Although our measurements were more macroscopic than these prior analyses, we did find that the amount of electrical activity correlated with increased LFP. In addition to EEG metrics, LFP was also associated with BFI, THC, and MAP. Thus, in the context of this study (where neurovascular interactions could be affected by anaesthesia and cardiac arrest) LFP was also correlated with systemic physiologic variation. LFP may also reflect information about cerebral autoregulation.[18] Despite these caveats, ALFF has been used as a biomarker for localized neuronal activity in psychiatric illness,[15,30–31] white matter injury,[32] and stroke.[17,33]

At least one prior study has examined LFP after cardiac arrest; van den Brule et al.[18] used TCD to assess CBF in adult cardiac arrest patients in the intensive care unit 6–72 h after cardiac arrest. Interestingly, the direction of the effect that we observed in predicting outcomes was the opposite of their study. They found that increased LFP was a good prognostic sign; LFP was higher in patients who survived to 72 h. This discrepancy might be explained by the fact that we assessed LFP in the first four hours after cardiac arrest, whereas they assess LFP 6–72 h after cardiac arrest. In the longer-term, increased neuronal activity is likely indicative of a recovering brain, and hence survival. However, assuming that LFP reflects brain activity, our results suggest that increased neuronal activity in the immediate post-recovery period may be detrimental. Our findings are consistent with the concept of preventing excess neuronal metabolism after cardiac arrest, which has been one motivation for therapeutic hypothermia, targeted temperature management, and other therapeutics.[34,35] In the TCD study, all patients received therapeutic hypothermia, which may explain their relatively low LFP measurements at the early time-points.

While we examined differences between the two CPR strategies, there were only minor differences between the two cohorts (limited by small sample sizes). Note that both CPR strategies were hemodynamically directed, providing high-quality CPR as compared to conventional depth-guided strategies.[19,20] Future studies using more disparate CPR strategies will investigate whether LFP or other biomarkers are associated with CPR quality.

Caution is necessary regarding interpretation of our results. The proposed relationship between neurologic activity and LFP depends on intact neurovascular coupling. It is unknown whether neurovascular coupling remains intact after cardiac arrest. Additionally, after ROSC, isoflurane was titrated as needed. The dosage range included doses known to allow continued neurovascular coupling as well as higher doses where neurovascular coupling is likely impaired. Furthermore, during periods of hemodynamic instability, MAP and CBF might be low (or high) enough to exhaust the ability to compensate, resulting in no cerebrovascular variation (i.e., minimal LFP) regardless of neurovascular coupling (of note, we did find that lower MAP and CBF were associated with lower LFP). As our electrical and CBF measurements were macroscopic, we were unable to study individual neurovascular units and assess whether neurovascular coupling remained intact at any given time.

While, increased LFP was associated with EEG metrics of neuronal activity, the EEG metrics themselves were not associated with the microdialysis outcomes. This result is consistent with prior human studies where the relationship between EEG and outcomes is unclear.[6,36] The global EEG parameters we used may not reflect the metabolic demand of individual neurons. LFP more closely approximates local field potentials than other electroencephalographic measures, which may explain its closer relationship with the outcome. Alternatively, this discrepancy may be an effect of sample size; the relationship between EEG parameters and LFP was assessed at every post-ROSC time point, while the comparison with microdialysis was conducted in 30-minute blocks. Since piglets differed in clinical course (e.g., anaesthestic exposure), we might expect time periods wherein neurovascular coupling was intact and LFP and EEG correlated with outcomes and other times periods wherein no correlation would be present. The mixed effects model can address some piglet-to-piglet differences, but an analysis of only on periods when neurovascular coupling was likely to be intact might show more associations.

Alternatively, the haemodynamic contributors to LFP might explain some of the association with outcomes. Especially during periods of impaired cerebral autoregulation, cerebral LFP may reflect variations in systemic physiology rather than local neurometabolic demand. However, the absolute value of CBF has not been associated with neurologic outcomes,[6,37] and haemodynamic measures were not consistently associated with microdialysis in our study. Future work should focus on the mechanism by which LFP reflects outcomes.

Our technique has several limitations. The DCS measure of absolute CBF is difficult to calibrate. For this reason, all data was normalized to baseline, which is not always clinically practicable. Improved absolute quantification of LFP may offer better results and more utility. In fMRI, adjustments to ALFF have been proposed, such as normalizing to the overall power in the BOLD signal.[38] Care must be taken in adapting such methods to optical techniques, where the sampling rate is much higher and aliasing of physiologic signals into low frequencies is not as prevalent. We plan to study methods to better normalize and quantify optical LFP.

Additionally, we assumed that changes in predictors would be associated with the microdialysis outcomes in the same 30-minute window. If neuronal injury takes longer to be reflected in the microdialysis biomarkers, then we might not capture that association. Given the limited number of piglets and time-points, we elected to not add an additional fitting variable to account for delay.

We assessed the reliability of LFP during the post-resuscitation period, but noninvasive measures of neuronal activity could potentially aid active resuscitation. Physiology-directed CPR improves outcomes in animal models of cardiac arrest,[19,20,39,40] and consensus guidelines recommend physiologic monitoring during CPR.[41–43] These techniques focus on systemic haemodynamics to increase coronary perfusion pressure and optimize the likelihood of ROSC.[19,20,39,41] Ideal biomarkers would not only optimize the chances of survival but also of favorable neurologic outcomes. Diffuse optical neuromonitoring holds promise to provide more direct measures of neuronal health and thus the adequacy of CPR.[21] LFP could supplement these metrics. However, DCS is strongly affected by motion artifacts; thus, we did not analyze LFP during CPR. Improved algorithms to remove motion artifacts in DCS will aid its use as a real-time clinical tool.

We were unable to assess LFP in DOS due to artifacts from intermittent acquisition. LFP would be straight-forward to calculate for DOS were its acquisition continuous, which is technically achievable. Assessment of LFP with DOS could aid resuscitation monitoring because DOS is less sensitive to motion artifacts and has been used during active resuscitation.[21] In the future, we intend to extend the present analysis to DOS as well as other optical neuroimaging techniques in animals and humans.

Conclusions

LFP in CBF measured by DCS is correlated with microdialysis biomarkers of neuronal injury during the first four hours after cardiac arrest in a piglet model. While interpreting LFP as reflective of neuronal activity must be done with caution pending further studies, these results offer promise that LFP analysis of optical neuromonitoring signals may provide a more direct biomarker of neuronal health to supplement measurements of cerebrovascular physiology or metabolism. Advanced optical neuromonitoring may improve diagnosis and prognosis in acutely ill patients.

Conflicts of interest

Authors disclose partial ownership of active relevant patents applications. Pending: WO 2021/091961 [TSK, WBB, RAB, RWM, AGY, DJL, TJK], WO2013/090658Al [AGY], PCT/US2012/069626 [AGY], PCT/US2015/017286 [AGY], PCT/US2015/017277 [AGY]. Granted: US8082015B2 [AGY]. No author currently receives royalties or payments from these patents. The authors do not have any further potential conflicts of interest relevant to the subject of this article at the time of submission. BRW, EJB, AL, JS, WPL, KA, JJ, JB, ND, SM, AR, YL, and KG declare no competing interests.

Funding

This work was supported by the National Institute of Neurological Disorders and Stroke (NINDS) [grant numbers K08-NS117897, R01-NS060653, R01-NS113945]; National Heart Lung and Blood Institute (NHLBI) [grant numbers T32-HL007915, R01-HL141386, K23-HL148541]; the National Institute of Biomedical Imaging and Bioengineering (NIBIB) [grant number P41-EB015893]; and the Children's Hospital of Philadelphia Frontier Program. Study sponsors had no involvement in the design, analysis, and or interpretation of this study; the writing of the manuscript; or the submission for publication.

Author contribution statement

BRW, TSK, RWM, WBB, RAB, AGY, DJL, and TJK contributed to the conception and design of the work. TSK, WBB, EJB, AL, JS, WPL, KA, JJ, JB, ND, SM, AR, YL, KG, and TJK acquired the data. BRW and TSK performed the analysis. BRW, TSK, RWM, WBB, RAB, AGY, DJL, and TJK contributed to data interpretation. BRW drafted the work, and TSK, RWM, WBB, AGY, DJL, RAB and TJK revised it critically. All authors gave final approval of the manuscript to be published and agreed to be accountable for all aspects of the work in ensuring that questions related to the accuracy or integrity of any part of the work are appropriately investigated and resolved.

Author details

[a]Division of Pediatric Cardiology, Department of Pediatrics, The Children's Hospital of Philadelphia and the Perelman School of Medicine at the University of Pennsylvania, United States[b]Division of Neurology, Department of Pediatrics, The Children's Hospital of Philadelphia and the Perelman School of Medicine at the University of Pennsylvania, United States [c]Department of Anesthesiology and Critical Care Medicine, The Children's Hospital of Philadelphia and the Perelman School of Medicine at the University of Pennsylvania, United States [d]Department of Physics and Astronomy, University of Pennsylvania, United States

REFERENCES

1. Holmberg MJ, Ross CE, Fitzmaurice GM, et al. Annual incidence of adult and pediatric in-hospital cardiac arrest in the United States. Circ Cardiovasc Qual Outcomes 2019;12:e005580.
2. Matos RI, Watson RS, Nadkarni VM, et al. Duration of cardiopulmonary resuscitation and illness category impact survival and neurologic outcomes for in-hospital pediatric cardiac arrests. Circulation 2013;127:442–51.
3. Girotra S, Nallamothu BK, Spertys JA, et al. Trends in survival after in-hospital cardiac arrest. New Eng J Med 2012;367:1912–20.
4. Holmberg MJ, Wiberg S, Ross CE, et al. Trends in survival after pediatric in-hospital cardiac arrest in the United States. Circulation 2019;140:1398–408.

5. Reis C, Akyol O, Araujo C, et al. Pathophysiology and the monitoring methods for cardiac arrest associated brain injury. Int J Mol Sci 2017;18:129.
6. Sinha N, Parnia S. Monitoring the brain after cardiac arrest: a new era. Curr Neurol Neurosci Rep 2017;17:62.
7. Cournoyer A, Iseppon M, Chauny JM, Denault A, Cossette S, Notebaert E. Near-infrared spectroscopy monitoring during cardiac arrest: a systematic review and meta-analysis. Acad Emerg Med 2016;23:851–62.
8. Raichle ME, Mintun MA. Brain work and brain imaging. Annu Rev Neurosci 2006;29:449–76.
9. Hillman EMC. Coupling mechanism and significance of the BOLD signal: a status report. Annu Rev Neurosci 2014;37:161–81.
10. Raichle ME. Two views of brain function. Trends Cog Sci 2010;14:180–90.
11. Al Nafisi B, van Amerom JFP, Forsey J, et al. Fetal circulation in left-sided congenital heart disease measured by cardiovascular magnetic resonance: a case-control study. J Cardiovasc Magn Reson 2013;15:65.
12. Fox MD, Raichle ME. Spontaneous fluctuations in brain activity observed with functional magnetic resonance imaging. Nat Rev Neurosci 2007;8:700–11.
13. Smith SM, Beckmann CF, Andersson J, et al. Resting-state fMRI in the human connectome project. Neuroimage 2013;80:144–68.
14. Power JD, Schlaggar BL, Petersen SE. Studying brain organization via spontaneous fMRI signal. Neuron 2014;84:681–96.
15. Zang YF, He Y, Zhu CZ, et al. Altered baseline brain activity in children with ADHD revealed by resting-state functional MRI. Brain Develop 2007;29:83–91.
16. Palacios EM, Sala-Llonch R, Junque C, et al. Resting-state functional magnetic resonance imaging activity and connectivity and cognitive outcome in traumatic brain injury. JAMA Neurol 2013;70:845–51.
17. White BR, Liao SM, Ferradal SL, Inder TE, Culver JP. Bedside optical imaging of occipital resting-state functional connectivity in neonates. Neuroimage 2012;59:2529–38.
18. van den Brule JMD, Vinke EJ, van Loon LM, van der Hoeven JG, Hoedemaekers CWE. Low spontaneous variability in cerebral blood flow velocity in non-survivors after cardiac arrest. Resuscitation 2017;111:110–5.
19. Morgan RW, Kilbaugh TJ, Shoap W, et al. A hemodynamic-directed approach to pediatric cardiopulmonary resuscitation (HD-CPR) improves survival. Resuscitation 2017;111:41–7.
20. Lautz AJ, Morgan RW, Karlsson M, et al. Hemodynamic-directed cardiopulmonary resuscitation improves neurologic outcomes and mitochondrial function in the heart and brain. Crit Care Med 2019;47:e241–9.
21. Ko TS, Mavroudis CD, Morgan RW, et al. Non-invasive diffuse optical neuromonitoring during cardiopulmonary resuscitation predicts return of spontaneous circulation. Sci Rep 2021;11:3828.
22. Friess SH, Sutton RM, Bhalala U, et al. Hemodynamic directed cardiopulmonary resuscitation improves short-term survival from ventricular fibrillation cardiac arrest. Crit Care Med 2013;41:2698–704.
23. Ko TS, Mavroudis CD, Baker WB, et al. Non-invasive optical neuromonitoring of the temperature-dependence of cerebral oxygen metabolism during deep hypothermic cardiopulmonary bypass in neonatal swine. J Cereb Blood Flow Metab 2020;40:187–203.
24. Mavroudis CD, Mensah-Brown KG, Ko TS, et al. Electroencephalographic response to deep hypothermic circulatory arrest in neonatal swine and humans. Ann Thorac Surg 2018;106:1841–6.
25. Vesoulis ZA, Gamble PG, Jain S, El Ters NM, Liao SM, Mathur AM. WU-NEAT: a clinically validated, open-source MATLAB toolbox for limited-channel neonatal EEG analysis. Comput Meth Prog Bio 2020;196:105716.
26. Rampil IJ, Weiskopf RB, Brown JG, et al. 1653 and isoflurane produce similar dose-related changes in the electroencephalogram of pigs. Anesthesiology 1988;69:298–302.
27. Tisdall MM, Smith M. Cerebral microdialysis: research technique or clinical tool. Brit J Anaesth 2006;97:18–25.
28. Logothetis NK, Pauls J, Augath M, Trinath T, Oeltermann A. Neurophysiological investigation of the basis of the fMRI signal. Nature 2001;412:150–7.
29. Pelled G, Goelman G. Different physiological MRI noise between cortical layers. Magn Reson Med 2004;52:913–6.
30. Turner JA, Chen H, Mathalon DH, et al. Reliability of low-frequency fluctuations in resting state fMRI in chronic schizophrenia. Psychiatry Res Neuroimaging 2012;201:253–5.
31. Xie B, Qiu MG, Zhang Y, et al. Alterations in the cortical thickness and the amplitude of low-frequency fluctuations in patients with post-traumatic stress disorder. Brain Res 2013;1490:225–32.
32. Smyser CD, Snyder AZ, Shimony JS, Blazey TM, Inder TE, Neil JJ. Effects of white matter injury on resting state fMRI measures in prematurely born infants. PLoS ONE 2013;8:e68098.
33. Bauer AQ, Kraft AW, Wright PW, Snyder AZ, Lee JM, Culver JP. Optical imaging of disrupted functional connectivity following ischemic stroke in mice. Neuroimage 2014;99:388–401.
34. Andersen LW, Holmberg MJ, Berg KM, Donnino MW, Granfeldt A. In-hospital cardiac arrest: a review. JAMA 2019;321:1200–10.
35. Callaway CW, Donnino MW, Fink EL, et al. 2015 American Heart Association guidelines update for cardiopulmonary resuscitation and emergency cardiovascular care, Part 8: Post-cardiac arrest care. Circulation 2015;132:S465–82.
36. Wijdicks EFM, Hijdra A, Young GB, Bassetti CL, Wiebe S. Practice parameter: prediction of outcome in comatose survivors after cardiopulmonary resuscitation (an evidence-based review). Neurology 2006;67:203–10.
37. Francoeur CL, Lee J, Dangayach N, Gidwani U, Mayer SA. Non-invasive cerebral perfusion monitoring in cardiac arrest patients: a prospective cohort study. Clin Neurol Neurosurg 2020;196:105970.
38. Zou QH, Zhu CZ, Yang Y, et al. An improved approach to detection of amplitude of low-frequency fluctuation (ALFF) for resting-state fMRI: fractional ALFF. J Neurosci Meth 2008;172:137–41.
39. Sutton RM, Friess SH, Naim MY, et al. Patient-centric blood pressure-targeted cardiopulmonary resuscitation improves survival from cardiac arrest. Am J Respir Crit Care Med 2014;190:1255–62.
40. Hamrick JL, Hamrick JT, Lee JK, Lee BH, Koehler RC, Shaffner DH. Efficacy of chest compressions directed by end-tidal CO2 feedback in a pediatric resuscitation model of basic life support. J Am Heart Assoc 2014;3:e000450.
41. Marquez AM, Morgan RW, Ross CE, Berg RA, Sutton RM. Physiology-directed cardiopulmonary resuscitation: advances in precision monitoring during cardiac arrest. Curr Opin Crit Care 2018;24:143–50.
42. Meaney PA, Bobrow BJ, Mancini ME, et al. Cardiopulmonary resuscitation quality: improving cardiac resuscitation outcomes both inside and outside the hospital: a consensus statement from the American Heart Association. Circulation 2013;128:417–35.
43. Topjian AA, Raymond TT, Atkins D, et al. 2020 American Heart Association Guidelines for cardiopulmonary resuscitation and emergency cardiovascular care, Part 4: Pediatric basic and advanced life support. Circulation 2020;142:S469–523.